

Spin Correlations in Production and Subsequent Decay of Neutralinos*

G. MOORTGAT-PICK[†]

*Institut für Theoretische Physik, Universität Würzburg, Am Hubland, D-97074 Würzburg, Germany,
Institut für Theoretische Physik, Universität Wien, Boltzmannngasse 5,
A-1090 Wien, Austria*

H. FRAAS[‡]

Institut für Theoretische Physik, Universität Würzburg, Am Hubland, D-97074 Würzburg, Germany

Abstract

We study the process $e^-e^+ \rightarrow \tilde{\chi}_1^0 \tilde{\chi}_2^0$ with the subsequent decay $\tilde{\chi}_2^0 \rightarrow \tilde{\chi}_1^0 \ell^+ \ell^-$ taking into account the complete spin correlations. We give the analytical formulae for the differential cross section and present numerical results for the lepton angular distribution and the distribution of the opening angle between the outgoing leptons for the LEP2 energy of $\sqrt{s} = 193$ GeV and for $\sqrt{s} = 500$ GeV. We examine three representative mixing scenarios in the MSSM and also study the influence of the common scalar mass parameter m_0 on the shape of the distributions. For the lepton angular distribution the effect of the spin correlations amounts to up to 20% for lower energies. We find that the opening angle distribution is suitable for distinguishing between higgsino-like and gaugino-like neutralinos. The shape of the lepton angular distribution is very sensitive to the mixing in the gaugino sector and to the value of m_0 . For higher energies it is also suitable for distinguishing between higgsino-like and gaugino-like neutralino.

PACS numbers : 12.60.Jv, 14.80.Ly, 13.88.+e, 13.10.+q, 13.30.Ce

*Work supported by the German Federal Ministry for Research and Technology (BMBF) under contract number 05 7WZ91P (0).

[†]e-mail: gudi@physik.uni-wuerzburg.de

[‡]e-mail: fraas@physik.uni-wuerzburg.de

I. INTRODUCTION

Although the Standard Model (SM) is extraordinarily successful for describing the electroweak phenomena, it has several theoretical shortcomings. The most severe of these deficiencies, the hierarchy problem, can satisfactorily be solved by the concept of supersymmetry (SUSY) broken at the TeV scale. This concept received a fresh impetus by the result that in a SUSY-GUT model the measured coupling constants evolved to high energies meet at a single point.

The most economical candidate for a realistic SUSY model with minimal gauge group $SU(3) \times SU(2) \times U(1)$ and with minimal content of particles is the Minimal Supersymmetric Extension of the Standard Model (MSSM). In this paper we consider its simplest version with the conserved quantum number R parity. Its implications include that SUSY particles can only be produced in pairs and the lightest supersymmetric particle (LSP) is stable and escapes detection. As usual we assume that this particle is the lightest neutralino $\tilde{\chi}_1^0$.

Among the new particles the charginos (the supersymmetric partners of the charged gauge and Higgs bosons) and the neutralinos (the partners of the neutral gauge and Higgs bosons) are of particular interest. As they are expected to be lighter than the gluino and in most scenarios lighter than the squarks and sleptons [1], [2], the next-to-lightest neutralino $\tilde{\chi}_2^0$ and the lightest chargino could be first observed in future experiments at e^+e^- -colliders. In particular the production of $\tilde{\chi}_1^0\tilde{\chi}_2^0$ pairs allows to study a wide region of the SUSY parameter space. Although in general chargino production is favoured by larger cross sections, in certain regions of the parameter space sizeable cross sections for the neutralino process can be expected [3]. Moreover it might be possible to discover SUSY by neutralino production if charginos are not accessible.

If new particles are discovered which are possible neutralino candidates, for a clear identification the complete investigation of their decay characteristics is indispensable. Neutralino decay widths and branching ratios have been thoroughly studied [4]. Angular distributions and angular correlations of the decay products can give valuable additional information on their composition from photino, zino and higgsino components.

Another interesting question is to see if angular distributions of decay products allow separation of neutralino production from chargino production.

Moreover, from decay angular distributions with complete spin correlations of the decaying particle one can infer the spin of the new particles.

Finally the identification of neutralinos would be completed by ascertaining their Majorana character. In Ref. [5,6] it is demonstrated that this is possible by means of the energy distributions of the decay leptons if the neutralinos are produced in collisions of polarized e^+e^- beams. The angular distributions of the decay products might, however, offer the possibility to prove the Majorana character if polarized beams are not available. Furthermore the angular distributions of the final leptons are suitable observables for studying CP-violation in supersymmetric models [6], [7].

The above mentioned reasons motivate a study of angular distributions in associated production of neutralinos and the subsequent decay of the next-to-lightest neutralino. Since angular distributions depend on the polarization of the parent particles one has to take into account spin correlations between production and decay.

In general quantum mechanical interference effects between various polarization states of the parent particles preclude simple factorization of the differential cross section into a production factor and a decay factor [8] unless the production amplitude is dominated by a single spin component [2]. However, in Ref. [9] it is shown that the factorization property holds for particles with spin provided that suitable Lorentz invariant variables are used. But this is not the case for angular distributions of the neutralino (or chargino) decay products in the laboratory frame. For energy distributions of the final particles in the laboratory frame the spin correlations are nevertheless usually ignored.

Heavy fermion production with subsequent decay was considered in Ref. [10]. Recently a Monte-Carlo generator for chargino production and decay including spin correlations was developed in Ref. [11].

In this paper we calculate the cross section of the process $e^+e^- \rightarrow \tilde{\chi}_1^0\tilde{\chi}_2^0$ and the subsequent direct leptonic decay, $\tilde{\chi}_2^0 \rightarrow \tilde{\chi}_1^0\ell^+\ell^-$. We give the analytical formulae of the differential cross section with complete spin correlations of the decaying neutralino. We study numerically the influence of these spin correlations on energy and angular distributions. The energy distributions are independent of spin correlations. However, for the lepton angular distributions for lower energies the effect of the spin correlations amounts to up to 20%. The shape of the lepton angular distribution is very sensitive to the mixing character in the gaugino sector and to the value of m_0 . For higher energies it is suitable for distinguishing between higgsino- and gaugino-like neutralino. We also analyze the opening angle distributions and show that at lower energies they are suitable for distinguishing between higgsino- and gaugino-like neutralinos. This will allow one to constrain the parameter space of the MSSM. We also consider the influence of the scalar mass parameter m_0 on the shape of distributions.

In Sec. 2 the general formalism is shown. In Sec. 2.1 the Lagrangian, couplings and Feynman diagrams are given, in Sec. 2.2 the spin-density formalism is presented, and in Sec. 2.3 the kinematics is given. In Sec. 3 we present the formulae for the differential cross section with complete spin correlations. Numerical results for the LEP2 energy

$\sqrt{s} = 193$ GeV and for $\sqrt{s} = 500$ GeV and a discussion are presented in Sec. 4.

II. GENERAL FORMALISM

A. The Feynman diagrams

In this section we show the Feynman diagrams and give the Lagrangian for the production process, $e^-(k_1)e^+(k_2) \rightarrow \tilde{\chi}_1^0(q_1)\tilde{\chi}_2^0(q_2)$, and for the direct leptonic decay, $\tilde{\chi}_2^0(q_2) \rightarrow \tilde{\chi}_1^0(p_1)\ell^+(p_2)\ell^-(p_3)$. The arguments k_1, k_2, q_1, q_2 and p_1, p_2, p_3 denote the momenta of the incoming electron, positron, the produced neutralinos $\tilde{\chi}_1^0, \tilde{\chi}_2^0$ and the outgoing neutralino $\tilde{\chi}_1^0$ and leptons ℓ^+, ℓ^- from the $\tilde{\chi}_2^0$ decay. Both the production and the decay process contain contributions from Z^0 exchange in the direct channel (s -channel) and from \tilde{e}_L and \tilde{e}_R exchange in the crossed channels (t -, u -channel). We introduce the kinematic variables:

$$s = (k_1 + k_2)^2, \quad \bar{s} = (p_2 + p_3)^2, \quad (1)$$

$$t = (k_2 - q_2)^2, \quad \bar{t} = (q_2 - p_2)^2, \quad (2)$$

$$u = (k_1 - q_2)^2, \quad \bar{u} = (q_2 - p_3)^2. \quad (3)$$

Channels referring to the decay are marked by a dash. The Feynman diagrams are shown in FIG.1.

From the interaction Lagrangian of the MSSM (in our notation and conventions we follow closely [12]),

$$\mathcal{L}_{Z^0\ell^+\ell^-} = -\frac{g}{\cos\theta_W} Z_\mu \bar{\ell} \gamma^\mu [L_\ell P_L + R_\ell P_R] \ell + \text{h.c.} \quad (4)$$

$$\mathcal{L}_{Z^0\tilde{\chi}_i^0\tilde{\chi}_j^0} = \frac{1}{2} \frac{g}{\cos\theta_W} Z_\mu \tilde{\chi}_i^0 \gamma^\mu [O_{ij}^L P_L + O_{ij}^R P_R] \tilde{\chi}_j^0 + \text{h.c.} \quad (5)$$

$$\mathcal{L}_{\ell\tilde{e}\tilde{\chi}_i^0} = g f_{\ell i}^L \bar{\ell} P_R \tilde{\chi}_i^0 \tilde{e}_L + g f_{\ell i}^R \bar{\ell} P_L \tilde{\chi}_i^0 \tilde{e}_R + \text{h.c.}, \quad i, j = 1, \dots, 4, \quad (6)$$

we obtain the couplings:

- $L_\ell = T_{3\ell} - e_\ell \sin^2 \theta_W, \quad R_\ell = -e_\ell \sin^2 \theta_W$
- $f_{\ell i}^L = -\sqrt{2} \left[\frac{1}{\cos\theta_W} (T_{3\ell} - e_\ell \sin^2 \theta_W) N_{i2} + e_\ell \sin\theta_W N_{i1} \right],$
 $f_{\ell i}^R = -\sqrt{2} e_\ell \sin\theta_W \left[\tan\theta_W N_{i2}^* - N_{i1}^* \right]$
- $O_{ij}^L = -\frac{1}{2} (N_{i3} N_{j3}^* - N_{i4} N_{j4}^*) \cos 2\beta - \frac{1}{2} (N_{i3} N_{j4}^* + N_{i4} N_{j3}^*) \sin 2\beta,$
 $O_{ij}^R = -O_{ij}^{L*}.$

In our case $i = 1, j = 2$ and we shall write $O_{12}^{L,R} = O^{L,R}$. Here $P_{L,R} = \frac{1}{2}(1 \mp \gamma_5)$, g is the weak coupling constant ($g = e/\sin\theta_W, e > 0$), and e_ℓ and $T_{3\ell}$ denote the charge and the third component of the weak isospin of the lepton ℓ . Furthermore $\tan\beta = \frac{v_2}{v_1}$, $v_{1,2}$ are the vacuum expectation values of the two neutral Higgs fields and N_{ij} is the unitary 4×4 matrix which diagonalizes the neutral gaugino-higgsino mass matrix in the basis $\tilde{\gamma}, \tilde{Z}, \tilde{H}_a^0, \tilde{H}_b^0$. Since we disregard in this paper CP violating phenomena the elements N_{ij} of the diagonalized matrix and the couplings can be chosen real. Then some of the neutralino mass eigenvalues may be negative and we shall write them in the form $\eta_i m_i$ with $m_i > 0, \eta_i = \pm 1$ [13]. The respective amplitudes for the Feynman diagrams are taken from Ref. [14].

B. Spin density matrix for production and decay

The differential cross section for the production $e^-(k_1)e^+(k_2) \rightarrow \tilde{\chi}_1^0(q_1)\tilde{\chi}_2^0(q_2)$ and the subsequent decay $\tilde{\chi}_2^0(q_2) \rightarrow \tilde{\chi}_1^0(p_1)\ell^+(p_2)\ell^-(p_3)$ is given by

$$d\sigma = \frac{1}{2\sqrt{\lambda(s, m_e^2, m_e^2)}} |T_{\lambda_{e^-} \lambda_{e^+}}^{\lambda_{\tilde{\chi}_1^0} \lambda_{\tilde{\chi}_2^0}}|^2 (2\pi)^4 \delta^{(4)}(k_1 + k_2 - q_1 - p_1 - p_2 - p_3) d\text{lips}(q_1, p_1, p_2, p_3), \quad (7)$$

where s is the cms-energy squared of the incoming e^- and e^+ and $\lambda(x, y, z) = x^2 + y^2 + z^2 - 2xy - 2xz - 2yz$ is the kinematical triangle function. All lepton masses are neglected. In Eq. (7) $\lambda_{e^-}, \lambda_{e^+}, \lambda_{\tilde{\chi}_1^0}$ and $\lambda_{\tilde{\chi}_2^0}, \lambda_{\ell^+}, \lambda_{\ell^-}$ label the helicities of the electron, positron and $\tilde{\chi}_1^0$ of the production process and the helicities of the $\tilde{\chi}_1^0, \ell^+, \ell^-$ of the decay

process, respectively. $d\text{lips}(q_1, p_1, p_2, p_3) = \frac{d^3 q_1}{(2\pi)^3 2q_1^0} \cdots \frac{d^3 p_3}{(2\pi)^3 2p_3^0}$ is the Lorentz invariant phase space element of the four final particles. The helicities $\lambda_{e^-}, \lambda_{e^+}$ of the initial particles are averaged because in this paper we consider the case of unpolarized beams. Since the polarization of the outgoing particles will not be measured, the helicities of the final particles $\lambda_{\bar{1}}$ and $\lambda_1, \lambda_+, \lambda_-$ have to be summed over. Therefore we suppress these helicity indices in the following and only display the helicity λ_2 of $\tilde{\chi}_2^0$.

The total width Γ_2 of the decaying neutralino $\tilde{\chi}_2^0$ is small compared to its mass m_2 . Therefore the amplitude T of the combined process is a coherent sum over all polarization states of the helicity amplitude P^{λ_2} for the production process times the helicity amplitude D_{λ_2} for the decay process and a pseudopropagator $\Delta_2 = \frac{1}{q_2^2 - m_2^2 + im_2 \Gamma_2}$ of $\tilde{\chi}_2^0$:

$$T = \Delta_2 P^{\lambda_2} D_{\lambda_2} \quad (8)$$

The amplitude squared for the combined process

$$|T|^2 = |\Delta_2|^2 \rho_P^{\lambda_2 \lambda_2'} \rho_{\lambda_2 \lambda_2}^D \quad (9)$$

is thus composed from the unnormalized spin density matrix

$$\rho_P^{\lambda_2 \lambda_2'} = P^{\lambda_2} P^{\lambda_2'}{}^* \quad (10)$$

of the neutralino $\tilde{\chi}_2^0$ and the decay matrix

$$\rho_{\lambda_2 \lambda_2}^D = D_{\lambda_2} D_{\lambda_2'}^* \quad (11)$$

for the respective decay channel. As in FIG.2 all helicity indices but that of the decaying neutralino are suppressed. Repeated indices are summed over.

Squaring the total amplitude one obtains interference terms between various helicity amplitudes. These terms preclude factorization in a production factor $\sum_{\lambda_2} |P^{\lambda_2}|^2$ times a decay factor $\sum_{\lambda_2} |D_{\lambda_2}|^2$ as for the case of spinless particles.

We use the general formalism to calculate the helicity amplitudes for production and decay of a particle with four-momentum p and mass m . Therefore we introduce three spacelike four-vectors s_μ^a , ($a = 1, 2, 3$) which together with p/m form an orthonormal set:

$$\frac{p}{m} \cdot s^a = 0 \quad (12)$$

$$s^a \cdot s^b = -\delta^{ab} \quad (13)$$

$$s_\mu^a \cdot s_\nu^a = -g_{\mu\nu} + \frac{p_\mu p_\nu}{m^2}. \quad (14)$$

A convenient choice for the explicit form of s^a is in a coordinate system where the direction of the three-momentum is $\hat{p} = (\sin \Theta \cos \Phi, \sin \Theta \sin \Phi, \cos \Theta)$ [15]:

$$s^{1\mu} = (0, -\sin \Phi, \cos \Phi, 0) \quad (15)$$

$$s^{2\mu} = (0, \cos \Theta \cos \Phi, \cos \Theta \sin \Phi, -\sin \Theta) \quad (16)$$

$$s^{3\mu} = \frac{1}{m}(|\vec{p}|, E\hat{p}). \quad (17)$$

Then in this frame of reference $s^{(1),(2)}$ and $s^{(3)}$ describe transverse and longitudinal polarization of the particle.

When computing the density matrices for production and decay, Eqs. (10), (11), we make use of the Bouchiat-Michel formulae [15]:

$$u(p, \lambda') \bar{u}(p, \lambda) = \frac{1}{2} [\delta_{\lambda\lambda'} + \gamma_5 \not{s}^a \sigma_{\lambda\lambda'}^a] (\not{p} + m) \quad (18)$$

$$v(p, \lambda') \bar{v}(p, \lambda) = \frac{1}{2} [\delta_{\lambda\lambda'} + \gamma_5 \not{s}^a \sigma_{\lambda'\lambda}^a] (\not{p} - m). \quad (19)$$

In the amplitude squared (Eq. (9)) the spin vectors s^a linearly enter the matrices ρ_P (Eq. (10)) and ρ^D (Eq. (11)). They induce by Eq. (14) the above mentioned quantum mechanical correlations between production and decay.

C. Kinematics and Phase Space

We split the phase space into the one for the production, $e^-(k_1)e^+(k_2) \rightarrow \tilde{\chi}_1^0(q_1)\tilde{\chi}_2^0(q_2)$, and the one for the three particle decay, $\tilde{\chi}_2^0(q_2) \rightarrow \tilde{\chi}_1^0(p_1)\ell^+(p_2)\ell^-(p_3)$. Then we obtain the differential cross section in the e^-e^+ -cms by integrating over the effective mass squared s_2 of the decaying neutralino $\tilde{\chi}_2^0$ [16]:

$$d\sigma = \frac{1}{8E_b^2} \int \frac{ds_2}{2\pi} \frac{W}{(s_2 - m_2^2)^2 + \Gamma_2^2 m_2^2} \times (2\pi)^4 \delta^{(4)}(q_1 + q_2 - k_1 - k_2) \frac{d^3 q_1}{(2\pi)^3 2E_1} \frac{d^3 q_2}{(2\pi)^3 2E_2} \times (2\pi)^4 \delta^{(4)}(p_1 + p_2 + p_3 - q_2) \frac{d^3 p_1}{(2\pi)^3 2E_1} \frac{d^3 p_2}{(2\pi)^3 2E_+} \frac{d^3 p_3}{(2\pi)^3 2E_-} \quad (20)$$

with $W = \rho_P^{\lambda_2 \lambda_2'} \rho_{\lambda_2' \lambda_2}^D$ (compare Eq. (9)). The energies of the produced $\tilde{\chi}_1^0, \tilde{\chi}_2^0$ are E_1, E_2 and those of $\tilde{\chi}_1^0, \ell^+$ and ℓ^- from the decay are denoted by \bar{E}_1, E_+ and E_- . E_b is the beam energy, m_2 is the mass of $\tilde{\chi}_2^0$ and the mass of $\tilde{\chi}_1^0$ is labeled by m_1 . Finally Θ_{M-} (Θ_{M+}) is the angle between the electron beam and the outgoing negatively (positively) charged lepton ℓ^- (ℓ^+) in the laboratory frame (FIG.3).

If the total width of the decaying particle $\tilde{\chi}_2^0$ is much smaller than its mass, $\Gamma_2 \ll m_2$, one can make the narrow width approximation $\frac{1}{(s_2 - m_2^2)^2 + m_2^2 \Gamma_2^2} \approx \frac{\pi}{m_2 \Gamma_2} \delta(s_2 - m_2^2)$ and one obtains for the differential cross section in the e^+e^- -cms, i.e. in the laboratory frame:

$$d\sigma = W \frac{1}{16(2\pi)^7} \frac{1}{|m_2| \Gamma_2} \frac{|\vec{q}_2|}{64E_b^3} \frac{E_+ E_- dE_- \sin \Theta d\Theta d\Phi d\Omega_+ d\Omega_-}{[E_2 - |\vec{q}_2| \cos \theta_{2+} - E_- (1 - \cos \Theta_{+-})]}. \quad (21)$$

Θ is the production angle of $\tilde{\chi}_2^0$, Φ describes the rotation around the electron beam axis, and $d\Omega_+$ ($d\Omega_-$) is the solid angle of ℓ_+ (ℓ_-).

In consequence of momentum conservation the energy E_+ is determined by E_- , the angles θ_{2-} (θ_{2+}) between ℓ^- (ℓ^+) and $\tilde{\chi}_2^0$, and the opening angle Θ_{+-} between the leptons:

$$E_+ = \frac{m_2^2 - m_1^2 - 2E_-(E_2 - |\vec{q}_2| \cos \theta_{2-})}{2[E_2 - |\vec{q}_2| \cos \theta_{2+} - E_- (1 - \cos \Theta_{+-})]}. \quad (22)$$

The possible region of the lepton energy E_- depends on the lepton decay angle θ_{2-} :

$$0 \leq E_- \leq \frac{m_2^2 - m_1^2}{2(E_2 - |\vec{q}_2| \cos \theta_{2-})}, \quad (23)$$

so that $E_+ = 0$, see Eq. (22), at the upper bound.

III. ANALYTICAL FORMULAE

In this section we give the analytical expressions for the product $W = \rho_P^{\lambda_2 \lambda_2'} \rho_{\lambda_2' \lambda_2}^D$ (compare Eq. (9)) of the density matrices for the production process, $e^-(k_1)e^+(k_2) \rightarrow \tilde{\chi}_1^0(q_1)\tilde{\chi}_2^0(q_2)$, and the direct leptonic decay, $\tilde{\chi}_2^0(q_2) \rightarrow \tilde{\chi}_1^0(p_1)\ell^+(p_2)\ell^-(p_3)$. Both the production and the decay process contain contributions from Z^0 exchange in the direct channel and from \tilde{e}_L and \tilde{e}_R exchange in the crossed channels (compare FIG.1).

The product W in Eq. (9) is a sum of contributions from the different production and decay amplitudes and their interference terms,

$$W = \sum_{ab,cd} W_{ab,cd}, \quad (24)$$

where the first pair a, b of indices refers to the production process, and the second pair c, d refers to the decay process. The pairs (ab) and (cd) run through all combinations of the values Z, L_t, L_u, R_t, R_u , where Z and L, R denote the exchanged particles Z^0 and \tilde{e}_L, \tilde{e}_R and $\tilde{\ell}_L, \tilde{\ell}_R$, respectively. In the case of slepton exchange the indices t, u denote the channel. Thus $W_{ZL_t, R_t R_u}$ is the contribution of the interference term to the production process from Z^0 -exchange

and \tilde{e}_L -exchange in the t-channel and the interference term to the decay process from $\tilde{\ell}_R$ -exchange in the \bar{t} -channel and $\tilde{\ell}_R$ -exchange in the \bar{u} -channel (FIG.1).

There are altogether 121 contributions $W_{ab,cd}$ which can be classified into 16 groups. We give one representative of each group and list the indices of the possible combinations. The other terms $W_{ab,cd}$ of this group are then obtained by substituting the propagator combination according to the pair of indices (see Eqs. (65)–(70)) and by substituting momenta and couplings and sign factors as given in TABLE I below. The substitutions of the momenta k_1, k_2, p_2, p_3 and of the couplings O^L, O^R, L, R also have to be performed in Eqs. (41)–(64). In the representative term the sign factors $\mu, \nu, \omega, \tau, v$ have the value +1.

For illustration we consider as an example $W_{L_t L_u, L_t L_t}$, which is the representative of Group 12. In order to get the contribution of $W_{R_t R_u, L_u L_u}$ one has to change the propagator combination $\Delta_L(t)\Delta_L(u)\Delta_L(\bar{t})\Delta_L(\bar{t}) \rightarrow \Delta_R(t)\Delta_R(u)\Delta_L(\bar{u})\Delta_L(\bar{u})$ and one has to substitute $\tilde{e}_L \rightarrow \tilde{e}_R$ in the production process and one has to substitute $\bar{t} \rightarrow \bar{u}$ in the decay process. When substituting $\tilde{e}_L \rightarrow \tilde{e}_R$, one has to change the sign factors ν, ω, v and the couplings according to the first line of TABLE I. Moreover, when substituting $\bar{t} \rightarrow \bar{u}$ one has to change the sign factors τ, v , the couplings and the momenta $p_2 \rightarrow p_3$ according to the fourth line of TABLE I.

Group 1 (1 term):

$$W_{ZZ,ZZ} = 32|\Delta_Z(s)|^2|\Delta_Z(\bar{s})|^2 \left\{ D1 \cdot P1 - D2_3 \cdot S1_2 + D2_2 \cdot S1_3 \right\} \quad (25)$$

Group 2 (4 terms):

Production: $(L_t Z), (R_t Z), (L_u Z), (R_u Z)$ Decay: (ZZ)

$$W_{L_t Z, ZZ} = 16\Delta_L(t)|\Delta_Z(\bar{s})|^2 \left\{ -\mu Re(\Delta_Z(s)) [D1 \cdot P2 + v(D2_3 \cdot S2_2 - D2_2 \cdot S2_3)] \right. \\ \left. + \nu v Im(\Delta_Z(s)) [D2_3 \cdot S6_2 - D2_2 \cdot S6_3] \right\} \quad (26)$$

Group 3 (4 terms):

Production: $(L_t L_t), (R_t R_t), (L_u L_u), (R_u R_u)$ Decay: (ZZ)

$$W_{L_t L_t, ZZ} = 8\Delta_L^2(t)|\Delta_Z(\bar{s})|^2 \left\{ (k_1 q_1)(k_2 q_2) D1 - v(D2_3 \cdot S3_2 - D2_2 \cdot S3_3) \right\} \quad (27)$$

Group 4 (2 terms):

Production: $(L_t L_u), (R_t R_u)$ Decay: (ZZ)

$$W_{L_t L_u, ZZ} = -8\Delta_L(t)\Delta_L(u)|\Delta_Z(\bar{s})|^2 \left\{ D1 \cdot P4 + v\eta_1 m_1 (D2_3 \cdot S4_2 - D2_2 \cdot S4_3) \right\} \quad (28)$$

Group 5 (4 terms):

Production: (ZZ) Decay: $(L_t Z), (R_t Z), (L_u Z), (R_u Z)$

$$W_{ZZ, L_t Z} = 16|\Delta_Z(s)|^2 \Delta_L(\bar{t}) \tau \left\{ Re(\Delta_Z(\bar{s})) \{ P1 \cdot D3 - v[D4 \cdot S1_2 - D5 \cdot S1_3] \} \right. \\ \left. - Im(\Delta_Z(\bar{s})) (R_e^2 - L_e^2) O^L \eta_1 m_1 [S7_2 \cdot P3_1 - S7_1 \cdot P3_2] \right\} \quad (29)$$

Group 6 (16 terms):

Production: $(L_t Z), (R_t Z), (L_u Z), (R_u Z)$ Decay: $(L_t Z), (R_t Z), (L_u Z), (R_u Z)$

$$W_{L_t Z, L_t Z} = 8\Delta_L(t)\Delta_L(\bar{t}) \tau \\ \cdot \left\{ -\mu Re(\Delta_Z(s)) Re(\Delta_Z(\bar{s})) [P2 \cdot D3 + v(D4 \cdot S2_2 - D5 \cdot S2_3)] \right. \\ + \omega v Im(\Delta_Z(s)) Re(\Delta_Z(\bar{s})) [D4 \cdot S6_2 - D5 \cdot S6_3] \\ - \nu Re(\Delta_Z(s)) Im(\Delta_Z(\bar{s})) L_e \eta_1 m_1 \\ \cdot [2\eta_2 m_2 O^R(k_1 q_1) S7_2 + \eta_1 m_1 O^L(k_1 q_2) S7_2 - \eta_1 m_1 O^L(k_2 q_2) S7_1] \\ \left. + Im(\Delta_Z(s)) Im(\Delta_Z(\bar{s})) L_e O^L \bar{L}_e \bar{O}^R m_1^2 [(p_2 q_2) S4_3 - (p_3 q_2) S4_2 + m_2^2 S5] \right\} \quad (30)$$

Group 7 (16 terms):

Production: $(L_t L_t), (R_t R_t), (L_u L_u), (R_u R_u)$ Decay: $(L_t Z), (R_t Z), (L_u Z), (R_u Z)$

$$W_{L_t L_t, L_t Z} = 4\Delta_L^2(t)\Delta_L(\bar{t})\tau \left\{ Re(\Delta_Z(\bar{s}))[(k_1 q_1)(k_2 q_2)D3 - v(D4 \cdot S3_2 - D5 \cdot S3_3)] \right. \\ \left. + \omega Im(\Delta_Z(\bar{s}))\eta_1 m_1 \eta_2 m_2 (k_1 q_1) S7_2 \right\} \quad (31)$$

Group 8 (8 terms):

Production: $(L_t L_u), (R_t R_u)$ Decay: $(L_t Z), (R_t Z), (L_u Z), (R_u Z)$

$$W_{L_t L_u, L_t Z} = -4\Delta_L(t)\Delta_L(u)\Delta_L(\bar{t}) \cdot \tau \left\{ Re(\Delta_Z(\bar{s}))[D3 \cdot P4 + v\eta_1 m_1 (D4 \cdot S4_2 - D5 \cdot S4_3)] \right. \\ \left. + \omega Im(\Delta_Z(\bar{s}))m_1^2[(k_1 q_2)S7_2 - (k_2 q_2)S7_1] \right\} \quad (32)$$

Group 9 (4 terms):

Production: (ZZ) Decay: $(L_t L_t), (R_t R_t), (L_u L_u), (R_u R_u)$

$$W_{ZZ, L_t L_t} = 8|\Delta_Z(s)|^2 \Delta_L^2(\bar{t})(p_1 p_3) \cdot \left\{ (p_2 q_2)P1 + v\eta_2 m_2 S1_2 \right\} \quad (33)$$

Group 10 (16 terms):

Production: $(L_t Z), (R_t Z), (L_u Z), (R_u Z)$ Decay: $(L_t L_t), (R_t R_t), (L_u L_u), (R_u R_u)$

$$W_{L_t Z, L_t L_t} = 4\Delta_L(t)\Delta_L^2(\bar{t})(p_1 p_3) \cdot \left\{ -\mu Re(\Delta_Z(s))[(p_2 q_2)P2 - v\eta_2 m_2 S2_2] - \nu v Im(\Delta_Z(s))\eta_2 m_2 S6_2 \right\} \quad (34)$$

Group 11 (16 terms):

Production: $(L_t L_t), (R_t R_t), (L_u L_u), (R_u R_u)$ Decay: $(L_t L_t), (R_t R_t), (L_u L_u), (R_u R_u)$

$$W_{L_t L_t, L_t L_t} = 2\Delta_L^2(t)\Delta_L^2(\bar{t}) \left\{ (p_1 p_3)(p_2 q_2)(k_1 q_1)(k_2 q_2) + v\eta_2 m_2 (p_1 p_3) S3_2 \right\} \quad (35)$$

Group 12 (8 terms):

Production: $(L_t L_u), (R_t R_u)$ Decay: $(L_t L_t), (R_t R_t), (L_u L_u), (R_u R_u)$

$$W_{L_t L_u, L_t L_t} = -2\Delta_L(t)\Delta_L(u)\Delta_L^2(\bar{t}) \left\{ (p_1 p_3)(p_2 q_2)P4 - v\eta_1 m_1 \eta_2 m_2 (p_1 p_3) S4_2 \right\} \quad (36)$$

Group 13 (2 terms):

Production: (ZZ) Decay: $(L_t L_u), (R_t R_u)$

$$W_{ZZ, L_t L_u} = 8|\Delta_Z(s)|^2 \Delta_L(\bar{t})\Delta_L(\bar{u}) \left\{ \eta_1 m_1 \eta_2 m_2 (p_2 p_3)P1 + v\eta_1 m_1 [(p_3 q_2)S1_2 - (p_2 q_2)S1_3] \right\} \quad (37)$$

Group 14 (8 terms):

Production: $(L_t Z), (R_t Z), (L_u Z), (R_u Z)$ Decay: $(L_t L_u), (R_t R_u)$

$$W_{L_t Z, L_t L_u} = 4\Delta_L(t)\Delta_L(\bar{t})\Delta_L(\bar{u}) \cdot \left\{ -\mu Re(\Delta_Z(s))[\eta_1 m_1 \eta_2 m_2 (p_2 p_3)P2 + v\eta_1 m_1 (-(p_3 q_2)S2_2 + (p_2 q_2)S2_3)] \right. \\ \left. + \nu v Im(\Delta_Z(s))\eta_1 m_1 [-(p_3 q_2)S6_2 + (p_2 q_2)S6_3] \right\} \quad (38)$$

Group 15 (8 terms):

Production: $(L_t L_t), (R_t R_t), (L_u L_u), (R_u R_u)$ Decay: $(L_t L_u), (R_t R_u)$

$$W_{L_t L_t, L_t L_u} = 2\Delta_L^2(t)\Delta_L(\bar{t})\Delta_L(\bar{u})\eta_1 m_1 \eta_2 m_2 (k_1 q_1) \cdot \left\{ (p_2 p_3)(k_2 q_2) + v[-(p_3 q_2)(k_2 p_2) + (p_2 q_2)(k_2 p_3)] \right\} \quad (39)$$

Group 16 (4 terms):

Production: $(L_t L_u), (R_t R_u)$

Decay: $(L_t L_u), (R_t R_u)$

$$W_{L_t L_u, L_t L_u} = -2\Delta_L(t)\Delta_L(u)\Delta_L(\bar{t})\Delta_L(\bar{u})\eta_1 m_1 \cdot \left\{ \eta_2 m_2 (p_2 p_3) P4 + v \eta_1 m_1 [-(p_3 q_2) S4_2 + (p_2 q_2) S4_3] \right\} \quad (40)$$

For the sake of a clear presentation of our analytical results we have introduced three groups of abbreviations. The first group refers to the production process:

$$P1 = (R_e^2 + L_e^2) \{ O^{L^2} [(k_1 q_1)(k_2 q_2) + (k_1 q_2)(k_2 q_1)] + O^L O^R \eta_1 m_1 \eta_2 m_2 (k_1 k_2) \} \quad (41)$$

$$P2 = 2L_e O^R (k_1 q_1)(k_2 q_2) + \eta_1 m_1 \eta_2 m_2 L_e O^L (k_1 k_2) \quad (42)$$

$$P3_1 = \eta_1 m_1 O^R (k_1 q_2) + \eta_2 m_2 O^L (k_1 q_1) \quad (43)$$

$$P3_2 = \eta_1 m_1 O^R (k_2 q_2) + \eta_2 m_2 O^L (k_2 q_1) \quad (44)$$

$$P4 = \eta_1 m_1 \eta_2 m_2 (k_1 k_2) \quad (45)$$

and the second group refers to the decay process:

$$D1 = (\bar{R}_e^2 + \bar{L}_e^2) \bar{O}^{L^2} \{ (p_1 p_3)(p_2 q_2) + (p_1 p_2)(p_3 q_2) + \eta_1 m_1 \eta_2 m_2 (p_2 p_3) \} \quad (46)$$

$$D2_2 = (\bar{R}_e^2 - \bar{L}_e^2) \bar{O}^{L^2} \{ \eta_1 m_1 (p_2 q_2) + \eta_2 m_2 (p_1 p_2) \} \quad (47)$$

$$D2_3 = (\bar{R}_e^2 - \bar{L}_e^2) \bar{O}^{L^2} \{ \eta_1 m_1 (p_3 q_2) + \eta_2 m_2 (p_1 p_3) \} \quad (48)$$

$$D3 = \bar{L}_e [2\bar{O}^L (p_1 p_3)(p_2 q_2) - \bar{O}^R \eta_1 m_1 \eta_2 m_2 (p_2 p_3)] \quad (49)$$

$$D4 = \bar{L}_e [\bar{O}^R \eta_1 m_1 (p_3 q_2) - 2\bar{O}^L \eta_2 m_2 (p_1 p_3)] \quad (50)$$

$$D5 = \bar{L}_e \bar{O}^R \eta_1 m_1 (p_2 q_2). \quad (51)$$

The third class is related to the spin correlations between production and decay and connects the momenta of both subprocesses:

$$S1_2 = (R_e^2 - L_e^2) \{ \eta_1 m_1 O^R O^L [(k_2 p_2)(k_1 q_2) - (k_1 p_2)(k_2 q_2)] + \eta_2 m_2 O^{L^2} [(k_2 q_1) \left(- (k_1 p_2) + \frac{(k_1 q_2)(p_2 q_2)}{m_2^2} \right) - (k_1 q_1) \left(- (k_2 p_2) + \frac{(k_2 q_2)(p_2 q_2)}{m_2^2} \right)] \} \quad (52)$$

$$S1_3 = (R_e^2 - L_e^2) \{ \eta_1 m_1 O^R O^L [(k_2 p_3)(k_1 q_2) - (k_1 p_3)(k_2 q_2)] + \eta_2 m_2 O^{L^2} [(k_2 q_1) \left(- (k_1 p_3) + \frac{(k_1 q_2)(p_3 q_2)}{m_2^2} \right) - (k_1 q_1) \left(- (k_2 p_3) + \frac{(k_2 q_2)(p_3 q_2)}{m_2^2} \right)] \} \quad (53)$$

$$S2_2 = -2\eta_2 m_2 L_e O^R (k_1 q_1) \left[- (k_2 p_2) + \frac{(k_2 q_2)(p_2 q_2)}{m_2^2} \right] + \eta_1 m_1 L_e O^L [(k_2 p_2)(k_1 q_2) - (k_1 p_2)(k_2 q_2)] \quad (54)$$

$$S2_3 = -2\eta_2 m_2 L_e O^R (k_1 q_1) \left[- (k_2 p_3) + \frac{(k_2 q_2)(p_3 q_2)}{m_2^2} \right] + \eta_1 m_1 L_e O^L [(k_2 p_3)(k_1 q_2) - (k_1 p_3)(k_2 q_2)] \quad (55)$$

$$S3_2 = \eta_2 m_2 (k_1 q_1) \left[- (k_2 p_2) + \frac{(k_2 q_2)(p_2 q_2)}{m_2^2} \right] \quad (56)$$

$$S3_3 = \eta_2 m_2 (k_1 q_1) \left[- (k_2 p_3) + \frac{(k_2 q_2)(p_3 q_2)}{m_2^2} \right] \quad (57)$$

$$S4_2 = (k_2 p_2)(k_1 q_2) - (k_1 p_2)(k_2 q_2) \quad (58)$$

$$S4_3 = (k_2 p_3)(k_1 q_2) - (k_1 p_3)(k_2 q_2) \quad (59)$$

$$S5 = (k_1 p_3)(k_2 p_2) - (k_1 p_2)(k_2 p_3) \quad (60)$$

$$S6_2 = L_e O^L \eta_1 m_1 [k_2 k_1 p_2 q_2] \quad (61)$$

$$S6_3 = L_e O^L \eta_1 m_1 [k_2 k_1 p_3 q_2] \quad (62)$$

$$S7_1 = \bar{L}_e \bar{O}^R [q_2 k_1 p_3 p_2] \quad (63)$$

$$S7_2 = \bar{L}_e \bar{O}^R [q_2 k_2 p_3 p_2] \quad (64)$$

with $[abcd] = \epsilon_{\mu\nu\rho\sigma} a^\mu b^\nu c^\rho d^\sigma$.

These terms, i.e. Eqs. (52)–(64), would be missing if we had assumed factorization of the differential cross section in production and decay.

For a better transparency all couplings originating from the decay process are marked by a dash. The indices are used in order to emphasize the symmetry between e^- and e^+ in the initial state and ℓ^- and ℓ^+ in the final state, respectively.

We have introduced the following products of propagators and coupling constants:

$$\Delta_Z(s) = \frac{g^2}{\cos^2 \theta_W} \cdot \frac{1}{s - m_Z^2 + im_Z \Gamma_Z} \quad (65)$$

$$\Delta_L(t) = \frac{g^2}{t - m_{\tilde{e}_L}^2} \cdot f_{\ell_1}^{L*} \cdot f_{\ell_2}^L \quad , \quad \Delta_R(t) = \frac{g^2}{t - m_{\tilde{e}_R}^2} \cdot f_{\ell_1}^{R*} \cdot f_{\ell_2}^R \quad (66)$$

$$\Delta_L(u) = \frac{g^2}{u - m_{\tilde{e}_L}^2} \cdot f_{\ell_1}^L \cdot f_{\ell_2}^{L*} \quad , \quad \Delta_R(u) = \frac{g^2}{u - m_{\tilde{e}_R}^2} \cdot f_{\ell_1}^R \cdot f_{\ell_2}^{R*} \quad (67)$$

and

$$\Delta_Z(\bar{s}) = \frac{g^2}{\cos^2 \theta_W} \cdot \frac{1}{\bar{s} - m_Z^2 + im_Z \Gamma_Z} \quad (68)$$

$$\Delta_L(\bar{t}) = \frac{g^2}{\bar{t} - m_{\tilde{e}_L}^2} \cdot \bar{f}_{\ell_2}^{L*} \cdot \bar{f}_{\ell_1}^L \quad , \quad \Delta_R(\bar{t}) = \frac{g^2}{\bar{t} - m_{\tilde{e}_R}^2} \cdot \bar{f}_{\ell_2}^{R*} \cdot \bar{f}_{\ell_1}^R \quad (69)$$

$$\Delta_L(\bar{u}) = \frac{g^2}{\bar{u} - m_{\tilde{e}_L}^2} \cdot \bar{f}_{\ell_2}^L \cdot \bar{f}_{\ell_1}^{L*} \quad , \quad \Delta_R(\bar{u}) = \frac{g^2}{\bar{u} - m_{\tilde{e}_R}^2} \cdot \bar{f}_{\ell_2}^R \cdot \bar{f}_{\ell_1}^{R*} \quad (70)$$

IV. NUMERICAL RESULTS AND DISCUSSION

A. Scenarios

Neutralinos are linear superpositions of the photino $\tilde{\gamma}$, the Zino \tilde{Z} and the two higgsinos \tilde{H}_a^0 and \tilde{H}_b^0 . The $\tilde{\gamma}$ and \tilde{Z} components only couple to the selectrons whereas the higgsino components couple to the Z^0 . The composition and the masses of the neutralino states depend on the three SUSY mass parameters M, M' (sometimes also called M_2 and M_1) and μ , whose values follow from the specific SUSY breaking mechanism, and on the ratio $\tan \beta = v_2/v_1$ of the vacuum expectation values of the Higgs fields. In order to reduce the number of parameters we shall assume $M' = \frac{5}{3} M \tan^2 \theta_W$ as suggested by grand unification [12]. The gaugino mass parameter M is related to the gluino mass by $M \approx 0.3 m_{\tilde{g}}$ [17] and the gluino mass is roughly given by $m_{\tilde{g}} \approx 2.4 m_{1/2}$ [18], where $m_{1/2}$ is the common gaugino mass at M_{GUT} ($M \approx 0.72 m_{1/2}$).

The masses of the sleptons are related to the SUSY parameters M and $\tan \beta$ and to the common scalar mass parameter m_0 at the unification point [17]:

$$m_{\tilde{\ell}_L}^2 = m_0^2 + 0.79 M^2 + m_z^2 \cos 2\beta (-0.5 + \sin^2 \theta_W) \quad (71)$$

$$m_{\tilde{\ell}_R}^2 = m_0^2 + 0.23 M^2 - m_z^2 \cos 2\beta \sin^2 \theta_W. \quad (72)$$

In order to illustrate the influence of the neutralino mixing and of the scalar mass m_0 we shall consider three representative scenarios which differ significantly in the nature of the two lowest mass eigenstates $\tilde{\chi}_1^0$ and $\tilde{\chi}_2^0$. The selectron masses are calculated for two values of the scalar mass m_0 , $m_0 = 90$ GeV and $m_0 = 200$ GeV. For the parameters of the Standard Model (SM) we take $m_Z = 91.19$ GeV, $\Gamma_Z = 2.49$ GeV, $\sin^2 \theta_W = 0.23$ [19] and $\alpha = 1/128$. We choose $\tan \beta = 2$. The parameters of our scenarios and the mass eigenvalues of the two lightest neutralinos, the light chargino and the selectrons are given in TABLE II. The width of the $\tilde{\chi}_2^0$ has been computed with the program of [20] (see TABLE II).

Notice that also in scenarios with $\mu < 0$ the branching ratio for the radiative decay is less than 0.5% in the examined region of parameter space [21].

The $\tilde{\gamma}$ and \tilde{Z} are mixtures of the \tilde{B} and the \tilde{W}_3 gauginos, $\tilde{\gamma} = \cos \theta_W \tilde{B} + \sin \theta_W \tilde{W}_3$, $\tilde{Z} = -\sin \theta_W \tilde{B} + \cos \theta_W \tilde{W}_3$. Therefore in TABLE III the components of the neutralino states are given in the basis $(\tilde{\gamma}, \tilde{Z}, \tilde{H}_a^0, \tilde{H}_b^0)$ and in the basis $(\tilde{B}, \tilde{W}_3, \tilde{H}_a^0, \tilde{H}_b^0)$.

In scenario A $\tilde{\chi}_1^0$ has a dominating photino component and $\tilde{\chi}_2^0$ has a dominating zino component, whereas in scenario B both neutralinos are nearly equal photino-zino mixtures. In the two scenarios A and B the $\tilde{\chi}_1^0$ is almost a pure

B-ino and the neutralino $\tilde{\chi}_2^0$ is nearly a pure \tilde{W}_3 -ino. In scenario C both neutralino states are dominated by strong higgsino components (TABLE III).

For the phase space integration (chosen relative accuracy 10^{-3}) we used the Monte-Carlo routine Vegas. The evaluation was made for cms-energies of $\sqrt{s} = 193$ GeV and $\sqrt{s} = 500$ GeV.

It can be derived from [9] that the total cross section factorizes, i.e. it is independent of the spin correlations. This fact has been used in our numerical calculations as a check for the phase space integration and the total cross sections are given in TABLE IV.

B. Lepton angular distributions

In this section we give numerical results for the angular distributions of ℓ^- with respect to the electron beam axis computed with complete spin correlations according to Eqs. (52)–(64). The angular distributions of ℓ^+ are obtained by substituting $\cos \Theta_{M-} \rightarrow -\cos \Theta_{M+}$.

In order to demonstrate the significance of the spin correlations we compare our results with those obtained from the assumption of factorization of the differential cross section into production and decay. As can be seen from FIGS.4–10 for all mixing scenarios and both values of the scalar mass m_0 the contribution of the spin correlations has the biggest effect in the forward and in the backward direction and vanishes in the direction perpendicular to the beam axis ($\cos \Theta_{M-} = 0$). The contribution of spin correlations in the forward direction has opposite sign of that in the backward direction. Their magnitude decreases with increasing energy.

Especially for lower energies the spin effect is sizeable in scenario A with a photino-like $\tilde{\chi}_1^0$ and a zino-like $\tilde{\chi}_2^0$ for both values of m_0 . For $\sqrt{s} = 193$ GeV ($\sqrt{s} = 500$ GeV) its magnitude amounts to about 20% (6%) in the forward and backward direction for both values of m_0 , $m_0 = 90$ GeV and $m_0 = 200$ GeV, FIG.4 (FIG.5). In both cases the contribution of the spin correlation is negative in the backward direction and positive in the forward direction.

A comparison with the results for the gaugino-like scenario B (FIG.6 and FIG.7) shows how sensitively the spin correlation effect depends on the gaugino-higgsino mixing and on the value of m_0 . It is noteworthy that although in both scenarios A and B the $\tilde{\chi}_1^0$ is B-ino-like and $\tilde{\chi}_2^0$ is \tilde{W}_3 -ino-like with, however, different phases of the \tilde{W}_3 -ino and B-ino admixture. For $\sqrt{s} = 193$ GeV and $m_0 = 90$ GeV (FIG.6) the magnitude of the spin effect is only 2% in the forward and in the backward direction whereas for $m_0 = 200$ GeV (FIG.7) it amounts to 10%. For higher energy $\sqrt{s} = 500$ GeV it is negligible (FIG.8).

It is remarkable that in the case of gaugino-like neutralinos the scalar mass m_0 crucially determines the shape of the angular distributions. This is most obvious for scenario B and $\sqrt{s} = 193$ GeV. For the smaller value $m_0 = 90$ GeV the angular distribution has a maximum nearly perpendicular to the beam direction and is almost FB symmetric, $A_{FB} = -0.8\%$ (compare TABLE V). The contribution of the spin correlations is positive in the backward direction and negative in the forward direction (FIG.6). Increasing the value of m_0 completely changes the shape of the angular distribution and for $m_0 = 200$ GeV it has a minimum in the backward hemisphere and the forward direction is favoured, $A_{FB} = +5.9\%$ (FIG.7). Now the contribution of the spin correlations is negative in the backward direction and positive in the forward direction.

In the higgsino-like scenario C both production and decay are dominated by Z^0 -exchange. Therefore the dependence on m_0 is considerably smaller and we give only numerical results for $m_0 = 90$ GeV. Here the contribution of spin correlations is negligible and the angular distribution is practically flat for $\sqrt{s} = 193$ GeV (FIG.9) and FB-symmetric, $A_{FB} = 0.07\%$, and for $\sqrt{s} = 500$ GeV with a minimum perpendicular to the beam direction and $A_{FB} = 0.11\%$ (FIG.10).

Notice however that a negligible FB-asymmetry is not an unequivocal signature for higgsino-like neutralinos. As can be seen from FIG.6 for scenario B with $m_0 = 90$ GeV the FB-asymmetry may also be small for gaugino-like neutralinos (see TABLE V). From FIGs.5, 8 and 10 we conclude that for higher energies far enough from threshold the lepton angular distribution is suitable for distinguishing between gaugino-like and higgsino-like neutralinos. For $\sqrt{s} = 500$ GeV the angular distribution is practically FB-symmetric with however a maximum for gauginos but a minimum for higgsinos perpendicular to the beam direction.

C. The lepton opening angle distribution

In contrast to the lepton angular distribution, the distribution of the opening angle between both leptons factorizes. Due to the Majorana character of the decaying neutralino the spin correlation terms are just cancelled by this partial phase space integration.

It is also noteworthy that in contrast to the lepton angular distributions, the distributions of the lepton opening angle are similar for both gaugino-like scenarios A and B (FIGs.11 and 12). Especially for $\sqrt{s} = 193$ GeV they differ, however, distinctively from that for higgsino-like neutralinos in scenario C (FIG.13).

In the case of gaugino-like neutralinos the distributions for $\sqrt{s} = 193$ GeV are rather flat (FIGs.11 and 12). Changing the scalar mass from $m_0 = 90$ GeV to $m_0 = 200$ GeV results in a reduction of the cross sections by a factor of approx. 3 in scenario A and by a factor of approx. 4 in scenario B. The shape of the distribution, however, remains essentially unchanged.

One should note that for the shape of the opening angle distributions the influence of varying the value of m_0 is much smaller than for the lepton angular distributions.

For higgsino-like neutralinos (FIG.13), the shape of the opening angle distribution for $\sqrt{s} = 193$ GeV is completely different from those of gaugino-like neutralinos. Here the lepton pairs are preferably emitted with small angles between them, approximately 66% of them with an opening angle between 0 and $\pi/2$.

With increasing energy the opening angle distribution shrinks more and more and for $\sqrt{s} = 500$ GeV it displays for both higgsino- and gaugino-like neutralinos a rather narrow peak at or near $\cos \Theta_{+-} = 1$. Obviously the distribution of the opening angle between the leptons is suitable to distinguish between gaugino- and higgsino-like neutralinos at lower energies.

D. Energy Distributions

Just as the opening angle distribution the energy distribution of the outgoing lepton factorizes. As a consequence of CP invariance (Sec. 2.1) and the Majorana character of the neutralinos the energy spectra of both leptons, ℓ^- and ℓ^+ , are identical [5].

In FIG.14 we give the energy distributions for scenario B for $m_0 = 90$ GeV and $m_0 = 200$ GeV and cms-energies of $\sqrt{s} = 193$ GeV and $\sqrt{s} = 500$ GeV. For all scenarios the position of the maximum is independent of the actual value of m_0 .

E. Summary

In this paper we have calculated the analytical expression for the differential cross section of the associated production of neutralinos, $e^- + e^+ \rightarrow \tilde{\chi}_1^0 + \tilde{\chi}_2^0$, and the subsequent direct leptonic decay, $\tilde{\chi}_2^0 \rightarrow \tilde{\chi}_1^0 + \ell^+ + \ell^-$, with complete spin correlations between production and decay. The angular and the energy distribution of the outgoing lepton as well as the distribution of the opening angle between both leptons have been computed for cms-energies of $\sqrt{s} = 193$ GeV and $\sqrt{s} = 500$ GeV. These distributions have been examined with regard to their dependence on spin correlations, on the neutralino mixing character and on the scalar mass parameter m_0 .

The quantum mechanical interference terms between the various polarization states of the decaying neutralino give rise to a strong effect in the lepton angular distribution with respect to the beam axis, whereas the opening angle distribution and the energy distribution are independent from these spin correlations.

For energies not too far above the threshold ($\sqrt{s} = 193$ GeV) the opening angle distribution turns out to be suitable for distinguishing between higgsino-like and gaugino-like neutralinos. However, it is rather insensible to variable mixing in the gaugino sector. Here the shape of the opening angle distribution only slightly depends on the scalar mass m_0 .

The lepton angular distribution, on the other hand, is for lower energies not only very sensitive to the mixing in the gaugino sector but also to the actual value of m_0 .

For energies far above threshold the shape of the lepton angular distribution is rather insensible to the mixing in the gaugino sector and to the value of m_0 . It is, however, extremely different for gaugino- and higgsino-like neutralinos and suitable for distinguishing between them.

If the neutralinos are gaugino-like, the effect of spin correlations in the angular distributions can be large amounting to about 20%. For higgsino-like neutralinos, on the contrary, the contribution of spin correlations is practically negligible.

The energy distributions and the distributions of the opening angle, finally, are independent from the spin correlations. Apart from the magnitude of the cross sections they are rather insensitive to the actual value of m_0 .

The clear structure of the analytical formulae presented here allows to include hadronic decays and to extend the investigations to cascade decays and to production and decay of, for instance, $\tilde{\chi}_2^0 \tilde{\chi}_2^0$ pairs. Concerning the hadronic decays, $\tilde{\chi}_2^0 \rightarrow \tilde{\chi}_1^0 q \bar{q}$, where the outgoing quarks develop two jets, we expect a similar shape of the opening angle

distribution between quark and antiquark. Thus, the two jets would be better separated for gaugino-like neutralinos than for higgsino-like neutralinos which prefer small opening angle.

These investigations as well as the inclusion of beam polarization and the results for the chargino process angular distributions will be discussed in a forthcoming paper with regard to the determination of SUSY parameters.

V. ACKNOWLEDGEMENT

We thank A. Bartl and W. Majerotto for many useful discussions. We are grateful to V. Latussek for his support in the development of the numerical program. This work was also supported by the Deutsche Forschungsgemeinschaft under contract Fr 1064/2-2 and the ‘Fond zur Förderung der wissenschaftlichen Forschung’ of Austria, Project No. P10843-PHY.

-
- [1] M.E. Peskin, Prog. Theor. Phys. Suppl. **123**, 507 (1996).
 - [2] J.L. Feng, M.J. Strassler, Phys. Rev. **D 55**, 1326 (1997).
 - [3] A. Bartl, H. Fraas, W. Majerotto, B. Mösslacher, Z. Phys. **C 55**, 257 (1992).
 - [4] S. Ambrosanio, B. Mele, Phys. Rev. **D 52**, 3900 (1995);
S. Ambrosanio, B. Mele, Phys. Rev. **D 53**, 2541 (1996).
 - [5] S.T. Petcov, Phys. Lett **B139**, 421 (1984).
 - [6] S.M. Bilenky, E.C. Christova, N.P. Nedelcheva, Bulg. Jour. of Phys. **13,4**, 283 (1986).
 - [7] Y. Kizukuri, N. Oshimo, Phys. Lett. **B 249**, 449 (1990).
 - [8] S. Kawasaki, T. Shirafuji, S.Y. Tsai, Progress of Th. Ph., **49/5**, 1656 (1973).
 - [9] D.A. Dicus, E.C.G. Sudarshan, X. Tata, Phys. Lett. **B 154**, 79 (1985).
 - [10] S. Gottlieb, T.J. Weiler, Phys.Rev. **D 32**, 1119 (1985);
S. Matsumoto, K. Tominaga, O. Terazawa, M. Biyajima, Int.J.Mod.Phys. **A 8**, 1153 (1993).
 - [11] C. Dionisi, K. Fujii, S. Giagu, T. Tsukamoto, in *Physics at LEP2*, CERN 96-01, eds. G. Altarelli, T. Sjöstrand, F. Zwirner, 337.
 - [12] H.E. Haber, G.L. Kane, Phys. Rep. **117**, 75 (1985).
 - [13] A. Bartl, H. Fraas, W. Majerotto, Phys. Rev. **D40**, 1594 (1989).
 - [14] A. Bartl, H. Fraas, W. Majerotto, Nucl.Phys. **B 278**, 1 (1986).
 - [15] H.E. Haber, in Proceedings of the 21st SLAC Summer Institute on Particle Physics, Stanford 1993.
 - [16] H. Pilkuhn, *The Interactions of Hadrons*, North-Holland Publishing Company, Amsterdam 1967.
 - [17] L.J. Hall, J. Polchinski, Phys. Lett. **B 152**, 335 (1985);
A. Bartl, M. Dittmar, W. Majerotto, in Proceedings of the Workshop e^+e^- Collisions at 500 GeV, ed. P. Zerwas, DESY **92-123B**, 603 (1992).
 - [18] A. Bartl et al., in Proceedings of the 1996 DPF/DPB Summer Study on New Directions for High-Energy Physics (Snowmass 96).
 - [19] Particle Data Group, Phys. Rev. **D 54**, 65 (1996).
 - [20] S. Hesselbach, H. Fraas, Phys. Rev. **D 55**, 1343 (1997)
 - [21] S. Ambrosanio, B. Mele, Phys. Rev. **D 55**, 1399 (1997).

FIG. 1. Feynman graphs for production and leptonic decay.

FIG. 2. The amplitude squared for the combined process including spin correlations is composed by the spin density matrix for the production and the decay matrix times the pseudopropagator Δ_2 squared (compare Eq. (9)).

FIG. 3. Configuration of momenta in the laboratory system. The lepton angular distribution refers to Θ_{M-} , the opening angle distribution to Θ_{+-} .

FIG. 4. Lepton angular distribution for $\sqrt{s} = 193$ GeV in scenario A for $m_0 = 90$ GeV with spin correlations fully taken into account (upper solid) and for assumed factorization (upper dotted); for $m_0 = 200$ GeV with spin correlations (lower solid) and for assumed factorization (lower dotted).

FIG. 5. Lepton angular distribution for $\sqrt{s} = 500$ GeV in scenario A for $m_0 = 90$ GeV with spin correlations fully taken into account (upper solid) and for assumed factorization (upper dotted); for $m_0 = 200$ GeV with spin correlations (lower solid) and for assumed factorization (lower dotted).

FIG. 6. Lepton angular distribution for $\sqrt{s} = 193$ GeV in scenario B for $m_0 = 90$ GeV with spin correlations fully taken into account (solid) and for assumed factorization (dotted).

FIG. 7. Lepton angular distribution for $\sqrt{s} = 193$ GeV in scenario B for $m_0 = 200$ GeV with spin correlations fully taken into account (solid) and for assumed factorization (dotted).

FIG. 8. Lepton angular distribution for $\sqrt{s} = 500$ GeV in scenario B for $m_0 = 90$ GeV with spin correlations fully taken into account (upper solid) and for assumed factorization (upper dotted); for $m_0 = 200$ GeV with spin correlations (lower solid) and for assumed factorization (lower dotted).

FIG. 9. Lepton angular distribution for $\sqrt{s} = 193$ GeV in scenario C for $m_0 = 90$ GeV with spin correlations fully taken into account (solid) and for assumed factorization (dotted).

FIG. 10. Lepton angular distribution for $\sqrt{s} = 500$ GeV in scenario C for $m_0 = 90$ GeV with spin correlations fully taken into account (solid) and for assumed factorization (dotted).

FIG. 11. Opening angle distribution in scenario A for $\sqrt{s} = 193$ GeV and $m_0 = 90$ GeV (upper solid) and $m_0 = 200$ GeV (lower solid); for $\sqrt{s} = 500$ GeV and $m_0 = 90$ GeV (upper dotted) and $m_0 = 200$ GeV (lower dotted);.

FIG. 12. Opening angle distribution in scenario B for $\sqrt{s} = 193$ GeV and $m_0 = 90$ GeV (upper solid) and $m_0 = 200$ GeV (lower solid); for $\sqrt{s} = 500$ GeV and $m_0 = 90$ GeV (upper dotted) and $m_0 = 200$ GeV (lower dotted).

FIG. 13. Opening angle distribution in scenario C for $\sqrt{s} = 193$ GeV and $m_0 = 90$ GeV (solid); for $\sqrt{s} = 500$ GeV and $m_0 = 90$ GeV (dotted).

FIG. 14. Energy distribution in scenario B for $\sqrt{s} = 193$ GeV and $m_0 = 90$ GeV (upper solid) and $m_0 = 200$ GeV (lower solid); for $\sqrt{s} = 500$ GeV and $m_0 = 90$ GeV (upper dotted) and $m_0 = 200$ GeV (lower dotted).

Production	μ	ν	ω	τ	v	Couplings	Momenta
$\tilde{e}_L \rightarrow \tilde{e}_R$	+1	-1	-1	+1	-1	$O^L \leftrightarrow O^R, L_e \leftrightarrow R_e$	
$t \rightarrow u$	-1	+1	-1	+1	-1	$O^L \leftrightarrow O^R$	$k_1 \leftrightarrow k_2$
decay							
$\tilde{\ell}_L \rightarrow \tilde{\ell}_R$	+1	+1	+1	+1	-1	$\bar{O}^L \leftrightarrow \bar{O}^R, \bar{L}_e \leftrightarrow \bar{R}_e$	
$\bar{t} \rightarrow \bar{u}$	+1	+1	+1	-1	-1	$\bar{O}^L \leftrightarrow \bar{O}^R$	$p_2 \leftrightarrow p_3$

TABLE I. Substitution rules for $W_{ab,cd}$, see Sec. 3.

	$\tan\beta$	M	μ	$\eta_1 m_1$	$\eta_2 m_2$	$\eta_{\tilde{\chi}_1^+} m_{\tilde{\chi}_1^+}$	$m_{\tilde{\ell}_L}^{90}$	$m_{\tilde{\ell}_R}^{90}$	$m_{\tilde{\ell}_L}^{200}$	$m_{\tilde{\ell}_R}^{200}$	$\Gamma_{\tilde{\chi}_2^0}^{90}$	$\Gamma_{\tilde{\chi}_2^0}^{200}$
A	2	84	-250	46	97	97	123	104	217	207	35.5	1.33
B	2	112	448	51	98	-97	139	110	226	210	15.0	0.74
C	2	215	-83	76	-109	97	214	114	279	228	23.6	23.7

TABLE II. Parameters M , μ and mass eigenvalues in GeV, total width of $\tilde{\chi}_2^0$ in keV. The superscripts denote the value of the scalar mass m_0 .

	$\tilde{\chi}_1^0$	$\tilde{\chi}_2^0$
	($\tilde{\gamma}$ \tilde{Z} \tilde{H}_a^0 \tilde{H}_b^0)	($\tilde{\gamma}$ \tilde{Z} \tilde{H}_a^0 \tilde{H}_b^0)
A	(+.94 -.33 -.08 -.08)	(-.35 -.89 -.16 -.23)
B	(+.79 -.60 +.11 +.07)	(-.62 -.76 +.17 +.10)
C	(-.17 +.22 -.19 +.94)	(-.05 +.29 -.92 -.26)
	(\tilde{B} \tilde{W}_3 \tilde{H}_a^0 \tilde{H}_b^0)	(\tilde{B} \tilde{W}_3 \tilde{H}_a^0 \tilde{H}_b^0)
A	(+.98 +.16 -.08 -.07)	(+.12 -.95 -.16 -.23)
B	(+.98 -.15 -.13 +.09)	(-.18 -.96 -.18 -.10)
C	(-.25 +.11 -.19 +.96)	(-.18 +.23 +.92 +.24)

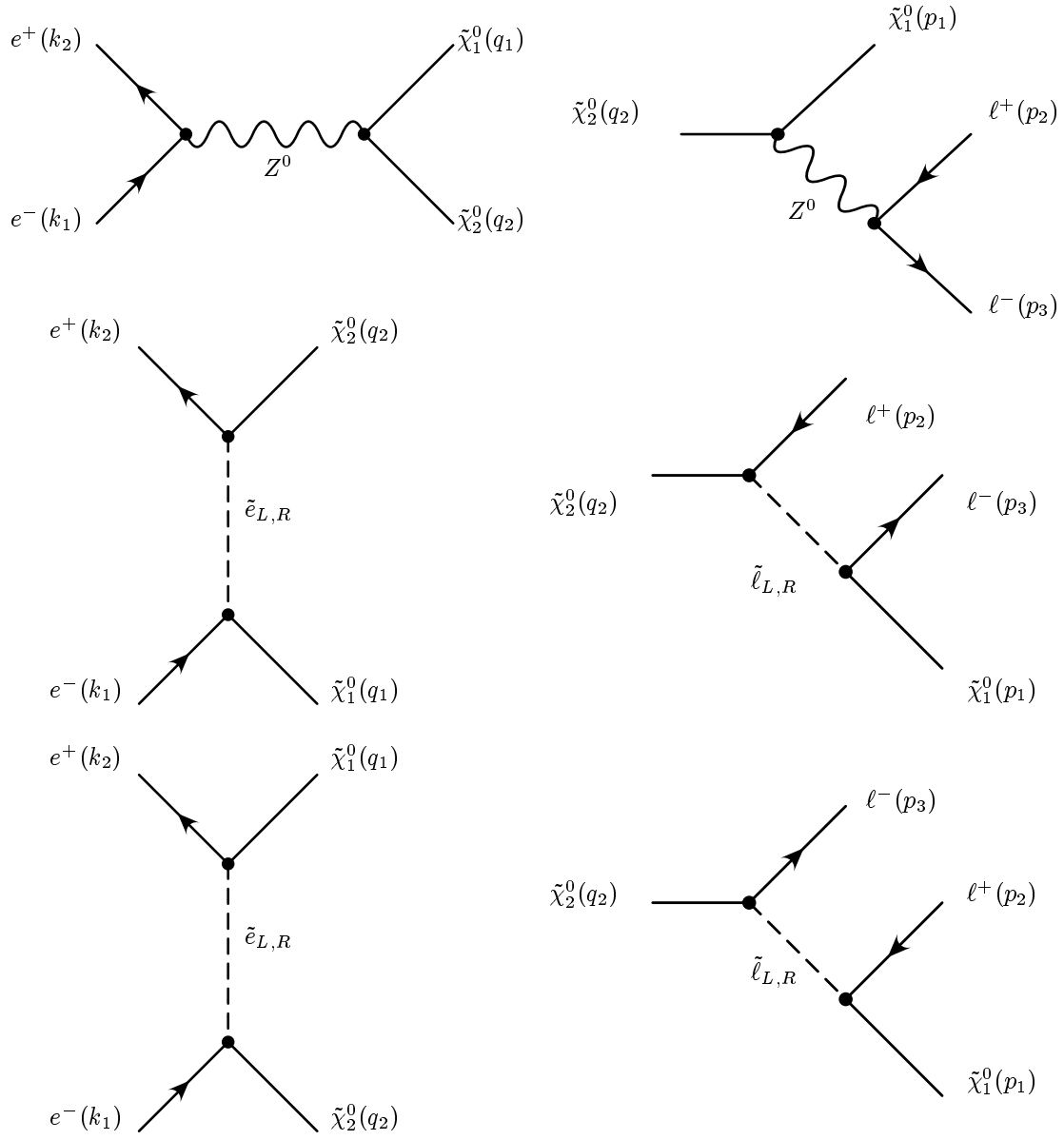
TABLE III. Neutralino eigenstates.

$\sigma(e^-e^+ \rightarrow \tilde{\chi}_1^0 \tilde{\chi}_2^0 \rightarrow \tilde{\chi}_1^0 \tilde{\chi}_1^0 \ell^+ \ell^-) \quad /fb$				
	$\sqrt{s} = 193 \text{ GeV}$		$\sqrt{s} = 500 \text{ GeV}$	
	$m_0 = 90 \text{ GeV}$	$m_0 = 200 \text{ GeV}$	$m_0 = 90 \text{ GeV}$	$m_0 = 200 \text{ GeV}$
A	38.9	11.1	32.7	21.6
B	10.0	2.5	10.9	6.1
C	23.3	23.4	6.0	6.1

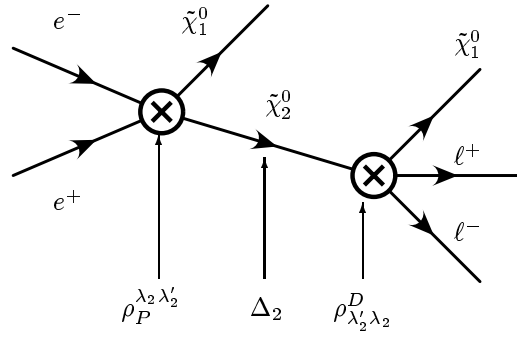
TABLE IV. Total cross sections for $e^-e^+ \rightarrow \tilde{\chi}_1^0 \tilde{\chi}_2^0$ and subsequent leptonic decay, $\tilde{\chi}_2^0 \rightarrow \tilde{\chi}_1^0 \ell^+ \ell^-$ for $\sqrt{s} = 193 \text{ GeV}$ and $\sqrt{s} = 500 \text{ GeV}$ with $m_0 = 90 \text{ GeV}$ and $m_0 = 200 \text{ GeV}$.

$A_{FB} = [\sigma(\cos \Theta_- > 0) - \sigma(\cos \Theta_- < 0)] / [\sigma(\cos \Theta_- > 0) + \sigma(\cos \Theta_- < 0)] \quad /[\%]$				
	$\sqrt{s} = 193 \text{ GeV}$		$\sqrt{s} = 500 \text{ GeV}$	
	$m_0 = 90 \text{ GeV}$	$m_0 = 200 \text{ GeV}$	$m_0 = 90 \text{ GeV}$	$m_0 = 200 \text{ GeV}$
A	10.2	11.6	2.3	3.0
B	-0.8	5.9	-0.3	1.8
C	0.07	0.11	-0.01	0.00

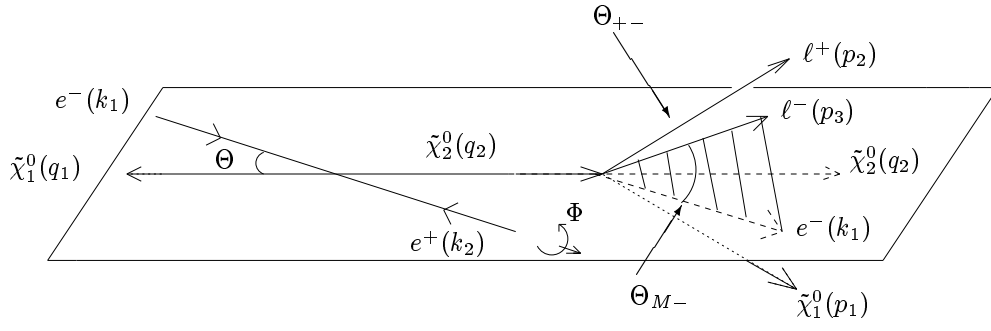
TABLE V. Forward-Backward-Asymmetry A_{FB} for $\sqrt{s} = 193 \text{ GeV}$ and $\sqrt{s} = 500 \text{ GeV}$ with $m_0 = 90 \text{ GeV}$ and $m_0 = 200 \text{ GeV}$.



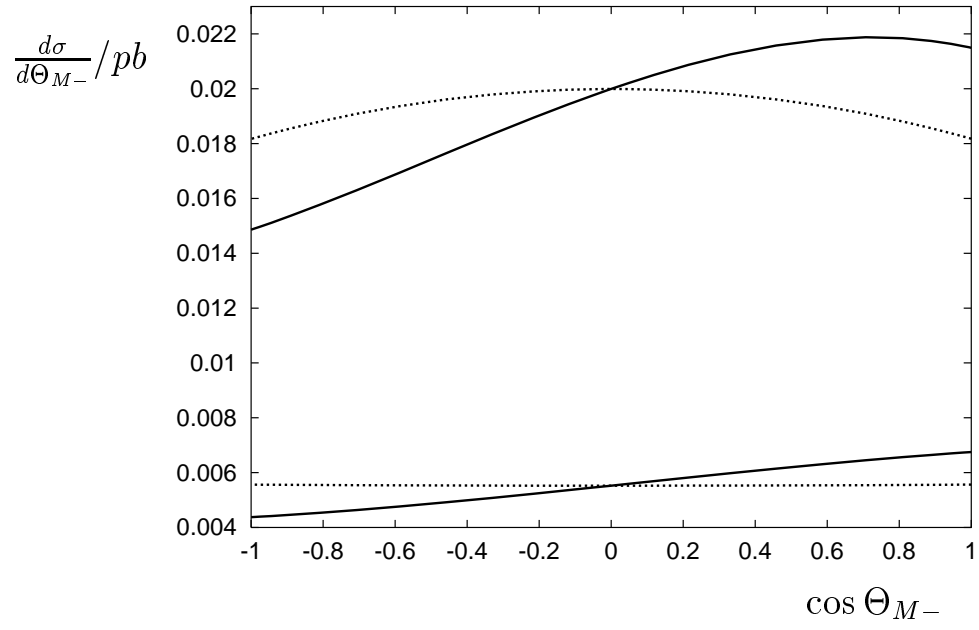
PRD, Moortgat-Pick/Fraas, FIG. 1



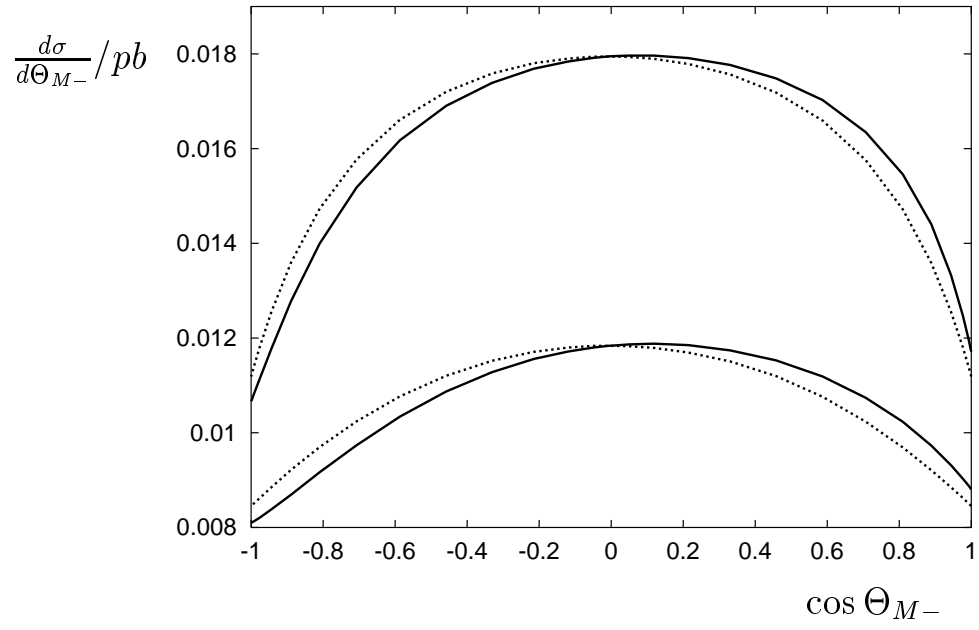
PRD, Moortgat-Pick/Fraas, FIG. 2



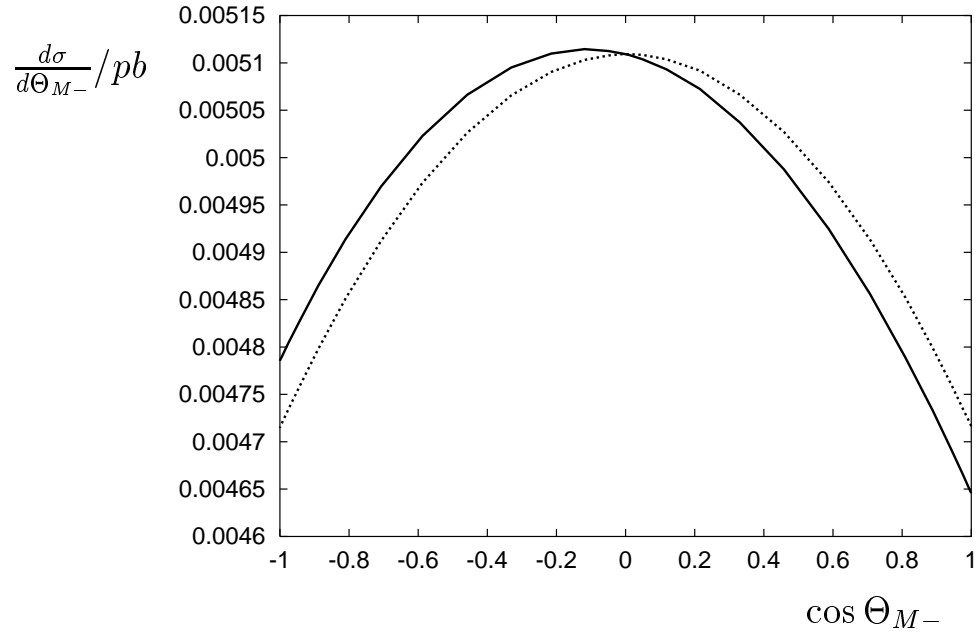
PRD, Moortgat-Pick/Fraas, FIG. 3



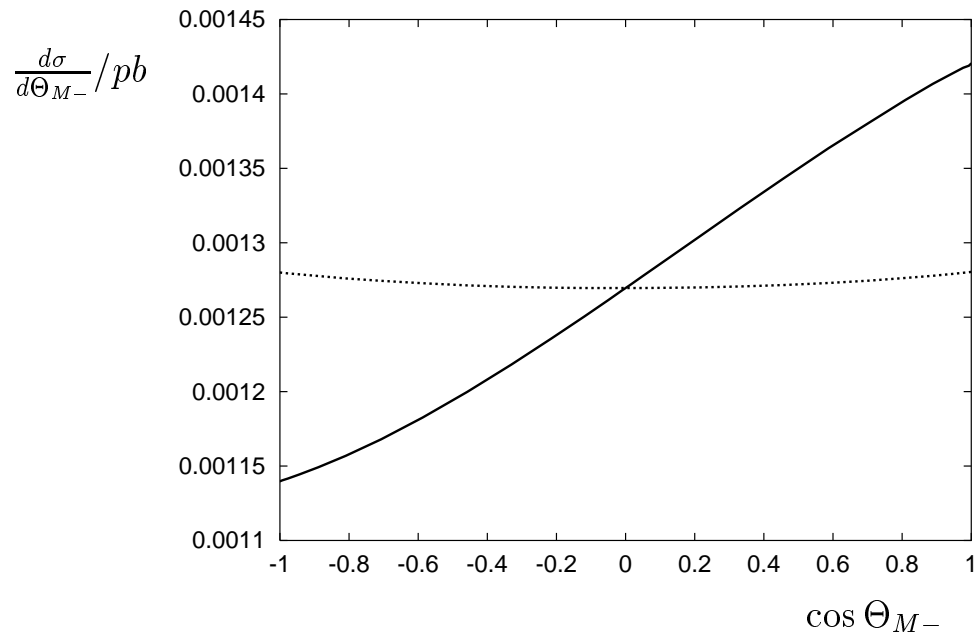
PRD, Moortgat-Pick/Fraas, FIG. 4



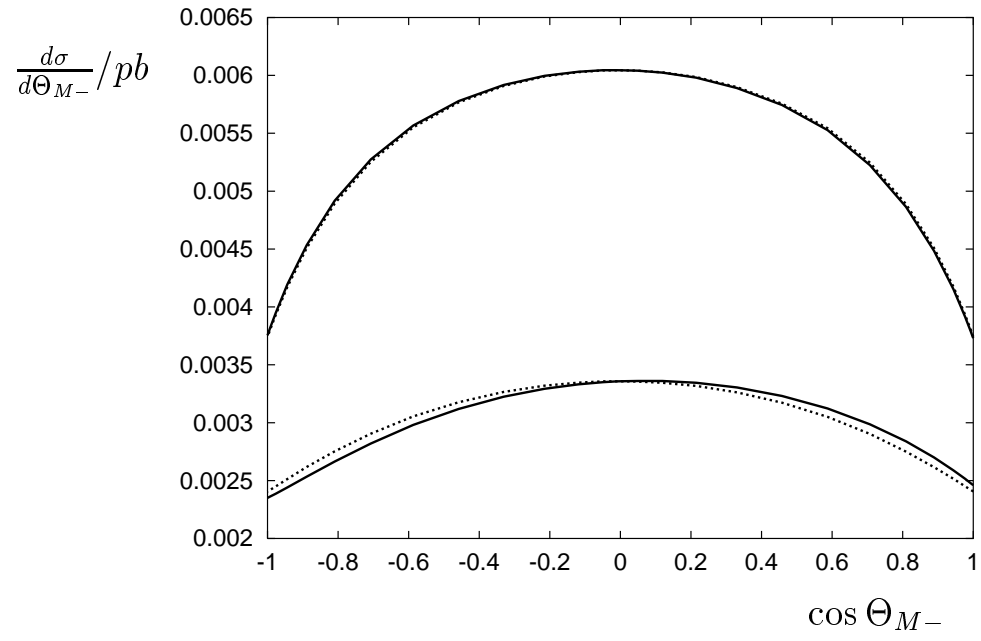
PRD, Moortgat-Pick/Fraas, FIG. 5



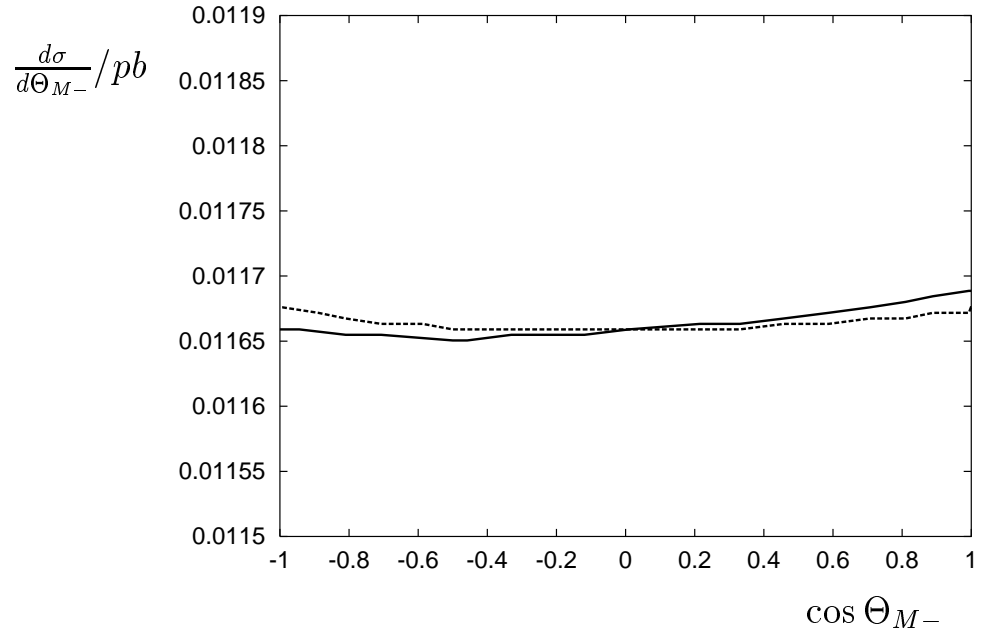
PRD, Moortgat-Pick/Fraas, FIG. 6



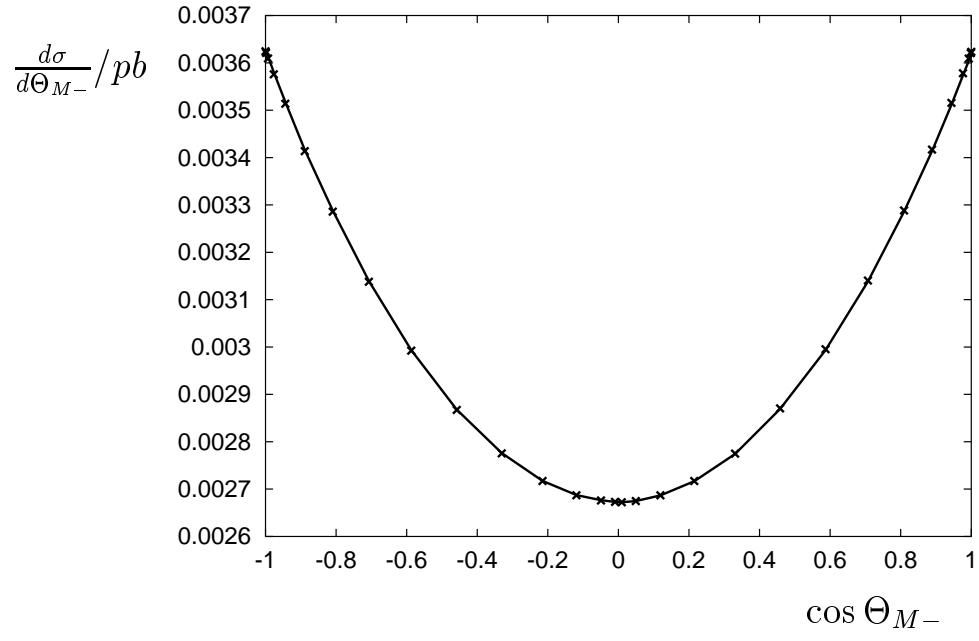
PRD, Moortgat-Pick/Fraas, FIG. 7



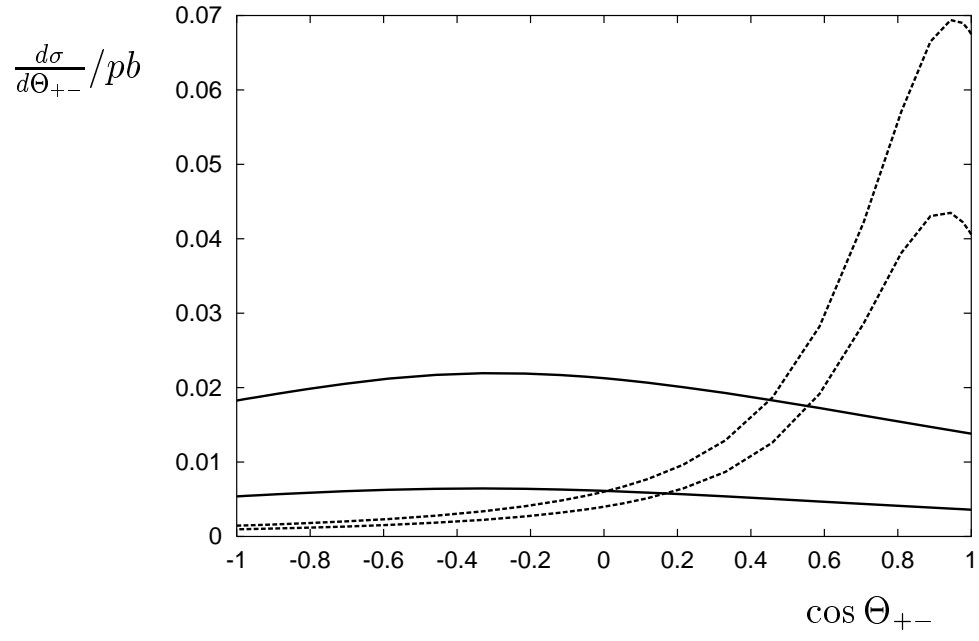
PRD, Moortgat-Pick/Fraas, FIG. 8



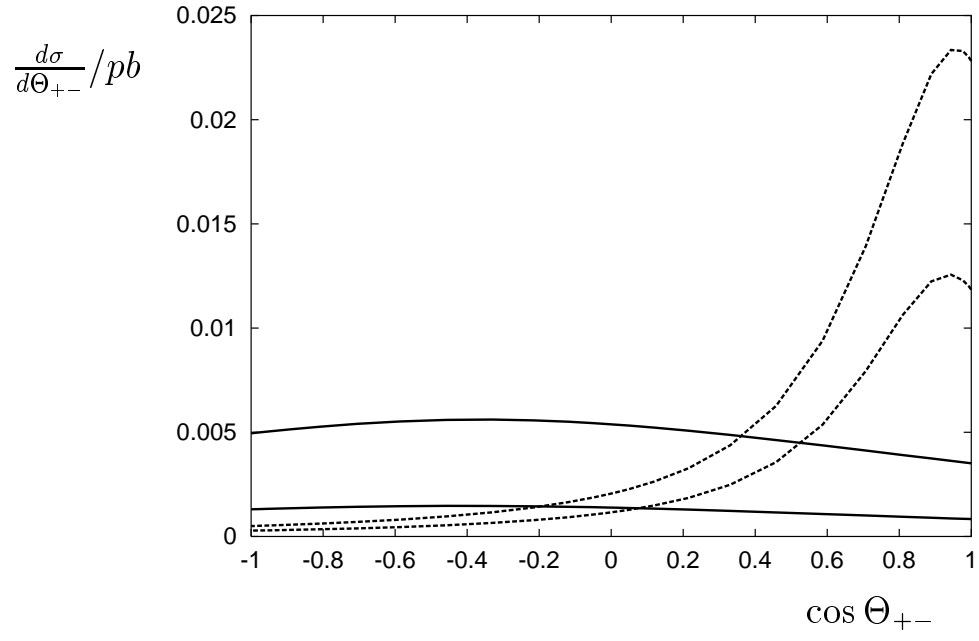
PRD, Moortgat-Pick/Fraas, FIG. 9



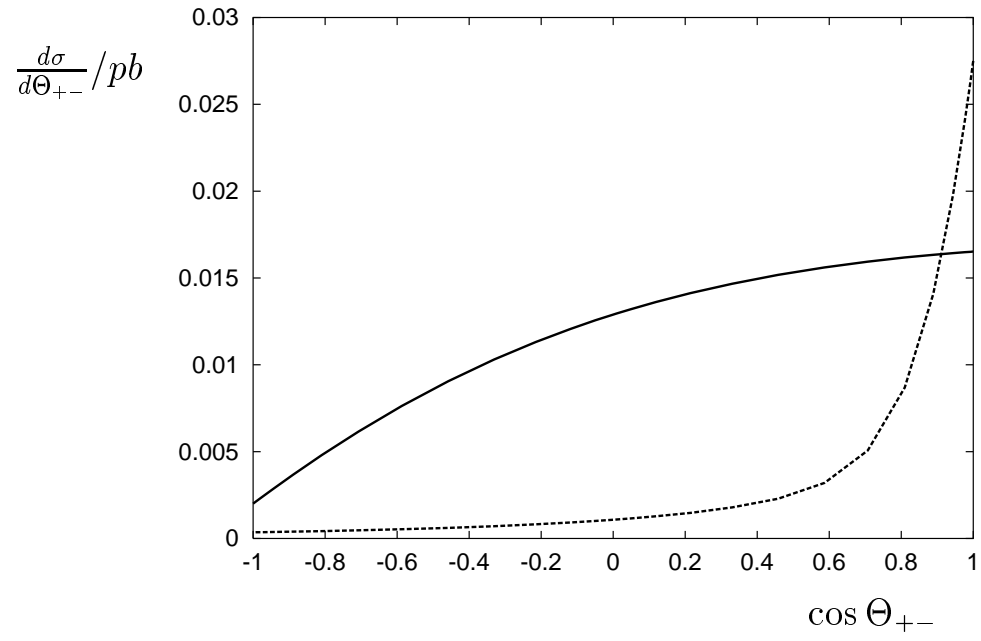
PRD, Moortgat-Pick/Fraas, FIG. 10



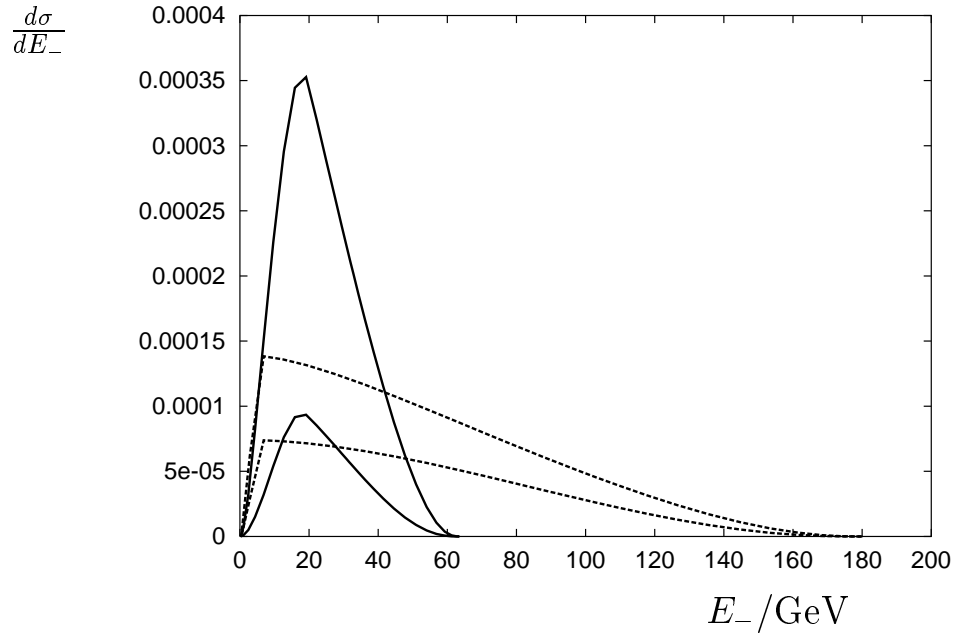
PRD, Moortgat-Pick/Fraas, FIG. 11



PRD, Moortgat-Pick/Fraas, FIG. 12



PRD, Moortgat-Pick/Fraas, FIG. 13



PRD, Moortgat-Pick/Fraas, FIG. 14